

MIT Open Access Articles

Development of a simple, compact, low-cost interference lithography system

The MIT Faculty has made this article openly available. **Please share** how this access benefits you. Your story matters.

Citation: Korre, Hasan et al. "Development of a Simple, Compact, Low-cost Interference Lithography System." *Journal of Vacuum Science & Technology B: Microelectronics and Nanometer Structures* 28.6 (2010): C6Q20. © 2010 American Vacuum Society

As Published: <http://dx.doi.org/10.1116/1.3504498>

Publisher: American Vacuum Society (AVS)

Persistent URL: <http://hdl.handle.net/1721.1/74116>

Version: Final published version: final published article, as it appeared in a journal, conference proceedings, or other formally published context

Terms of Use: Article is made available in accordance with the publisher's policy and may be subject to US copyright law. Please refer to the publisher's site for terms of use.



Development of a simple, compact, low-cost interference lithography system

Hasan Korre^{a)} and Corey P. Fucetola

Department of Electrical Engineering and Computer Science, Massachusetts Institute of Technology, Cambridge, Massachusetts 02139

Jeremy A. Johnson

Department of Chemistry, Massachusetts Institute of Technology, Cambridge, Massachusetts 02139

Karl K. Berggren

Department of Electrical Engineering and Computer Science, Massachusetts Institute of Technology, Cambridge, Massachusetts 02139

(Received 12 July 2010; accepted 27 September 2010; published 2 December 2010)

Interference lithography (IL) has proven itself to be an enabling technology for nanofabrication. Within IL, issues of spatial phase distortion, fringe stability, and substrate development have been explored and addressed. However, IL tools are still unnecessarily expensive, large, and complex. To address these issues, the authors previously built a simple IL tool that used a blue laser diode to produce ~ 300 nm pitch structures. The resulting patterned areas ($\sim \text{mm}^2$) were limited by both the temporal and spatial coherence of the laser. Here, the authors report on the advancement of their low-cost interference lithography tool that makes use of newly available blue laser diodes and a simplified spatial filter to print larger-area ($\sim \text{cm}^2$) patterns. With this configuration, the authors have designed and implemented a small-footprint ($\sim 0.2 \text{ m}^2$) Lloyd's mirror IL tool that can be assembled for less than ~ 6000 USD. © 2010 American Vacuum Society.

[DOI: 10.1116/1.3504498]

I. INTRODUCTION

Interference lithography (IL) has proven its usefulness in the fabrication of periodic nanostructures for photonic crystals, diffraction gratings, magnetic domains in recording media, and nanochannels in microfluidics.¹ Recently, IL has also been adapted to create templates for self-assembly,² to fabricate nanoimprint molds,³ to verify new lithographic techniques such as absorbance modulation,^{4,5} and to influence the placement of extracellular matrix by osteoblasts.⁶ However, typical IL tools that produce periodic nanostructures have an $\sim 2.8 \text{ m}^2$ footprint, require significant maintenance, and cost more than 100 000 USD. As a result, research groups have become interested in tackling the problem of low-cost interference lithography. For example, Byun and Kim were able to use an AlInGaN blue laser diode to make 290 nm pitch gratings and 750 nm pitch two-dimensional rod and hole patterns for ~ 15 000 USD.⁷ Their setup required a spatial filter (which requires training and skill to align) and a 2.2 m beam expansion length.

We address the demand for a small, simple, low-cost IL tool by implementing a Lloyd's mirror that produces periodic nanostructures with a minimum of maintenance, space, and money. The Lloyd's mirror interference lithography tool uses a simple and rigid setup to produce one- and two-dimensional patterns.⁸ We previously presented our initial results,⁹ where we used a simplified version of the Lloyd's mirror that contained only the essential elements and was sufficient for the $\sim 1 \text{ mm}^2$ patterning of one-dimensional

nanostructures. Although we demonstrated the feasibility of low-cost interference lithography, the diffractive structures produced by this tool displayed nonuniformities—visible to the naked eye—due to non-idealities in the spectrum of the laser. We were able to capture the spatial variation of the nonuniformities by measuring the first-order diffracted power from our substrates. Here, we address the temporal and spatial incoherence of our previous setup while maintaining the goals of simplicity and compactness. We made use of a blue laser diode with optical feedback and have built a simplified spatial filter. These improvements allow $\sim \text{cm}^2$ one- and two-dimensional periodic patterns to be printed, and we present images of our results.

II. TOOL DESIGN

Figure 1 composes the schematics of our previous and current setups. A 5 mW, 405 nm laser diode module emitted an expanding beam of light that was aligned to a simple mirror/substrate chuck. The laser diode current, power, and temperature were not stabilized nor was there a spatial filter; moreover, the pitch of the resulting one-dimensional nanostructures was not adjustable. In contrast, Fig. 1(b) shows the improved interference lithography system. Improvements include the use of a commercially available 12 mW, 405 nm laser diode package with an integrated collimation and volume holographic grating (VHG) optical feedback system, a shutter/spatial filter assembly that does not require micrometers, and a rotation stage having arcminute accuracy.

The diode package we used was obtained at a substantially lower cost than more commonly used gas lasers and

^{a)}Electronic mail: hkorre@mit.edu

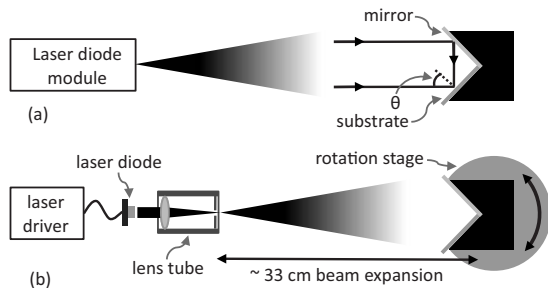


FIG. 1. Schematics of our previous and new interference lithography setups in Lloyd's mirror configuration. (a) Our previous setup included a 405 nm laser diode module and an inexpensive mirror/substrate chuck. (b) The new setup includes a laser driver, a collimated grating feedback laser diode, a spatial filter consisting of a lens and pinhole inside a lens tube system, an inexpensive mirror/substrate chuck, and a rotation stage. Rotation of the mirror/substrate chuck allows the pitch to be modified. The beam expansion length is ~ 33 cm. Note that the reflected beam traveling from the mirror to the substrate is shown perpendicular to the optical axis for clarity and is not perpendicular for the general case. Also, the incident beam is depicted as a plane wave for clarity, an approximation that becomes more accurate as the beam expansion length increases.

does not require periodic maintenance or frequent alignment. In contrast to grating- or etalon-based external cavity diode laser systems,¹⁰ the embedded VHG makes our IL system easier to configure because it provides an optical feedback system without requiring any external cavity alignment.¹¹ The diode was mounted on a rotation mount to allow the polarization of the beam to be set with the E-field pointing perpendicular to the plane-of-incidence of the substrate and to allow the laser source to be attached to the beam shutter and spatial filter. Additionally, the laser current was controlled with driver circuitry, but still no effort was made to control the laser's power or temperature.

We built a low-cost spatial filter from a lens aligned through a lens tube to a pinhole that is mounted on a ± 1 mm travel, 100 threads-per-inch (TPI) XY lens translating mount. The 0.25 numerical aperture (NA) lens was mounted within the lens tube, and the translating mount was attached collinear to the lens tube. The lens' position was adjusted with 40 TPI retaining rings to bring the pinhole close to the focal plane, and the 100 TPI screws on the translating mount provided enough control to align the 5 μm diameter pinhole to the focal spot of the lens. This design made use of the passive linearity and stability of a lens tube to eliminate the tip-tilt stage of more elaborate spatial filters. Beyond the spatial filter, the beam freely expands until it reaches the substrate stage. The distance between the spatial filter and the substrate stage is only 33 cm.

The substrate/mirror mount consisted of a 90° angle machinist's v-block connected to a rotation stage with a micrometer controlled travel. Rotation of the v-block allowed control of the pitch of the periodic patterns. On one side of the v-block was mounted a 3.5 \times 5.0 cm² aluminum first-surface mirror with a multilayer film of dielectrics on top. On the other side was placed the substrate. Both were adhered to the machinist's block with double-sided adhesive carbon tape. Together, the proposed tool minimized size, complex-

ity, and cost. The tool had a footprint of only 0.2 m². Setup, maintenance, and alignment were simple. Lastly, the tool costs less than 6000 USD.

III. PROCEDURES

In our previous work,⁹ it was observed that there was a strong correlation between the fringe visibility calculated from the power spectrum and the measured first-order diffraction efficiency from fabricated gratings. We surmised that the multimode power spectrum was causing a low spatial frequency (~ 1 mm² scale) modulation of the $\sim \lambda/2$ -period standing wave intensity pattern that was then recorded in a photoresist. Therefore, we should be able to eliminate the beating by exposing test substrates with a narrow-spectrum laser and measuring the first-order diffraction efficiency along the direction on the substrate that starts at zero path-length-difference and runs perpendicular to the mirror.

To test the performance of the improved design, we fabricated test substrates, exposed them in the tool, developed and imaged the resulting gratings in a top-down view, measured their diffraction efficiency, then transferred the grating patterns and imaged the cross sections of the gratings again.

Test substrates consisted of a trilayer resist stack as described in Ref. 9 and developed in Ref. 12. The three layers consisted of (1) a bottom layer of 200 or 303.1 nm of Barli (AZ Electronic Materials) antireflection coating (ARC), (2) 25 nm of evaporated silicon oxide (SiO_x), and (3) 180 nm of PFI-88 (Sumitomo Chemicals), a positive tone photoresist. In between the SiO_x and photoresist, a layer of hexamethyldisilazane was spin coated to promote adhesion of the photoresist to the SiO_x.

Lithographic exposures were carried out at a 42.5 mA laser diode drive current. Before exposure, we measured the incident power over a 0.71 cm² area at the center of the v-block and found the power to be ~ 100 μW . Using the incident intensity (incident power/detector area) and the clipping dose (the dose at which the resist goes from unexposed to exposed), the exposure time can be derived. Exposure times for different angles were calculated using the formula

$$t = \frac{D_0}{I_p T (1 + R) \cos \theta},$$

where t is the exposure time, D_0 is the clipping dose, I_p is the incident laser intensity, T is the proportion of light transmitted through the resist, R is the fraction of light reflected into the resist from the antireflection coating layer, and θ is the beam angle at the substrate (as depicted in Fig. 1).¹³ From test exposures, we observed the clipping dose to be ~ 52 mJ/cm².

Two-dimensional patterns required a double-exposure technique: a first exposure was done to provide half the clipping dose, after which the substrate is rotated at 90° and the remaining half of the dose is applied. After exposure, substrates were developed in liquid tetramethylammonium hy-

dioxide (TMAH, 2.4% wt CD-26, Rohm & Haas Electronic Materials),^{14,15} rinsed in de-ionized water, and then blown dry with N₂ gas.

Before inspection in a scanning electron microscope (SEM), less than 5 nm of Au/Pd was sputter deposited onto the substrates. The SEM was a DSM 982 Gemini from Zeiss SMT with an in-lens secondary-electron detector. All images were taken at 5 keV electron energy at a 4 mm working distance.

The spectrum of our laser was measured with a Spectrex spectrometer with 5.5 pm spectral resolution at the same laser diode drive current as was used during exposures.

Automated scans of the first-order diffracted power from fabricated gratings were carried out using a LABVIEW program to control the laser driver, a translation stage, and a power meter simultaneously. A laser beam (405 nm wavelength) passed through a 200- μm -wide slit. The beam was then diffracted by a fabricated grating and detected by the power meter to measure the diffracted power. The translation stage scanned the grating at a step size of 0.1 mm.

With portions of the samples that were not already imaged, a standard process was used to transfer patterns from the photoresist to the ARC. Two etch runs were required for the pattern transfer. In the first etch step, we performed reactive ion etching with CHF₃ gas at 200 V for 120 s, with the power ranging between 67 and 82 W during the etch. Then in the second etch, we used 16 sccm (sccm denotes cubic centimeter per minute at STP) of helium and 8 sccm of oxygen gas at 250 V for 315 s at a power of 115–121 W. The pressure for both etch runs was 10 mTorr.

IV. RESULTS

In our previous work, we deduced that our patterning area was limited by our laser spectrum.⁹ Here, we present measured spectral data of a new laser. With this laser, we are able to accomplish the following results: (1) our new patterns were not limited to 1 mm² area, (2) the system can control the pitch of the resulting pattern, and (3) the system has the ability to form two-dimensional patterns.

We measured the spectrum of the blue laser diode with an optical feedback. The spectrum data had a full width at half maximum ($\Delta\lambda$) of 59.6 pm. The calculated coherence length of the laser ($\sim\lambda^2/\Delta\lambda$) was estimated to be ~ 2.7 mm. Measurement of the laser diode spectrum from the vendor¹⁶ showed a spectrum with $\Delta\lambda=2.9$ pm. The coherence length from this measurement was estimated to be ~ 5.7 cm. The measurement taken from the vendor is more consistent with the observed results, namely, the ability to fabricate diffractive nanostructures that extend continuously over a 1 cm² area. We have not identified the specific cause of the discrepancy, but we assume that our measurement was limited in some way.

Figure 2 presents the measured first-order diffraction efficiency from a grating fabricated with the laser. The diffraction efficiency lacks the $\sim\text{mm}$ scale beating pattern seen in Ref. 9 and has a sharp drop off, which is believed to be due to the incident intensity variation produced by the spatial

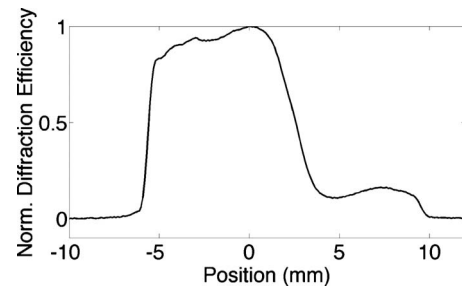


Fig. 2. Measured first-order diffraction efficiency from a fabricated grating. The measurements were done by a home-built, automated setup. The diffraction efficiency is notably missing the $\sim\text{mm}$ scale beating pattern that was observed in Ref. 9.

filter. Notably, the normalized diffraction efficiency is continuously greater than 0.5 over 8 mm. This sample was observed to diffract light from an area larger than 1 cm².

Figure 3 shows periodic nanostructures in the photoresist. Figures 3(a)–3(c) are a set of three gratings at different pitches. The pitches, which were measured in a SEM, were $p_a=230.0\pm 0.2$ nm, $p_b=291.9\pm 0.5$ nm, and $p_c=559\pm 2.5$ nm. The angle of exposure is related to the period by the equation,

$$p = \frac{\lambda}{2 \sin \theta}.$$

Using the peak wavelength of the measured laser spectrum (404.9 nm), we find the exposure angles to be $\theta_a=61.7^\circ$, $\theta_b=43.9^\circ$, and $\theta_c=21.2^\circ$. The duty cycle (the ratio of feature width to pitch) was also measured in the SEM. They were $w_a=40.5\%$, $w_b=55.8\%$, and $w_c=54.2\%$.

Figure 3(d) shows a two-dimensional rod pattern produced with Lloyd's mirror. The pitch of the pattern was

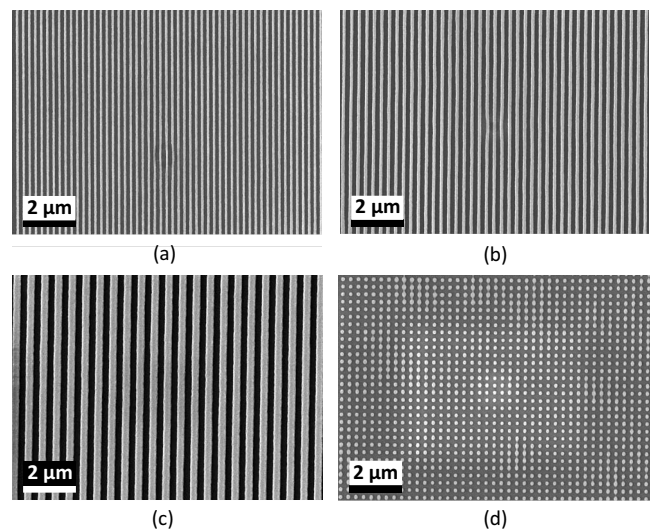


Fig. 3. Scanning-electron-micrograph images of patterns, produced by the system described in this article, in the positive photoresist. The images were taken at 5 keV electron energy and a working distance of 4 mm. The periods of the patterns are (a) 230, (b) 292, (c) 559, and (d) 314 nm. The figure displays the tool's ability to change the pitch of one-dimensional gratings and to produce two-dimensional patterns.

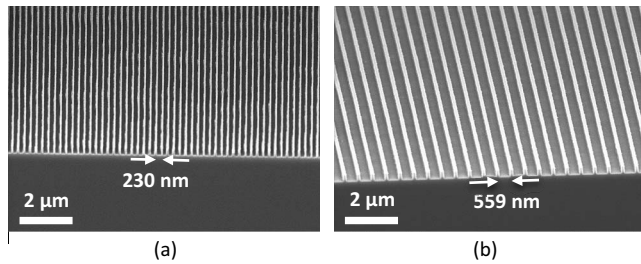


FIG. 4. One-dimensional periodic patterns transferred into the ARC layer. The scanning-electron-microscope images were taken at a 5 keV electron energy and a 4 mm working distance. The periods were (a) 230 and (b) 559 nm.

314.3 ± 0.6 nm. There was an observable bridging between some of the posts. We attribute this bridging to a spatial intensity variation that may be due to the incoherent reflection from our mirror edges or may originate from the imperfections of the spatial filter.

Figure 4 shows grating lines pattern-transferred into the antireflection coating. Figure 4(a) is of 230 nm pitch and is the same substrate as in Fig. 3(a). Figure 4(b) has a pitch of 559 nm and is the same substrate as in Fig. 3(c).

V. DISCUSSION AND SUMMARY

A systematic investigation of the limitation of the tool needs to be carried out. Although the laser has been able to produce continuous, diffractive nanostructures over 1 cm^2 , investigation should be done to determine the largest patternable area possible with the tool. The plateau in the diffraction efficiency is indicative of an exposure area that is limited by the uniformity of the incident beam intensity. Users can expand the incident beam spot area in three ways: (1) by increasing the beam expansion length, (2) by making use of a smaller pinhole, and (3) by maximizing the NA of the lens within the spatial filter. All three of these approaches would require compromising the goals of the tool. The tool would not be compact if it required a long beam expansion length. Also a long expansion length and a smaller pinhole (i.e., $1 \text{ }\mu\text{m}$) decrease the tool's simplicity by decreasing the incident beam power and therefore requiring longer exposure times. Lastly, alignment difficulty depends on the size of either the focused beam spot (i.e., $\sim 1/\text{NA}$) or the pinhole depending on which is smaller. Therefore, either the spot size or the pinhole diameter must be kept relatively large compared to the passive alignment tolerances of the system.

In addition, pattern uniformity maybe an issue for some applications. Four issues affect pattern uniformity: (1) fringe contrast, (2) average dose, (3) hyperbolic phase distortion, and (4) standing waves. As shown in Ref. 17, the fringe contrast and average dose affect the linewidth of features and, as a result, the duty cycle. The fringe contrast will vary over the 1 cm^2 area because of the short coherence length of our laser. The uniformity of the average dose over an area of 1 cm^2 is limited by the short expansion length of our beam and the pinhole size. Also, in this experiment the power was not controlled, limiting the accuracy in targeting a specific

dose. It has been shown—using a similar resist stack—that the dose margin (the average dose that can develop one-dimensional nanostructures) for this type of setup spans at least from 0.83 to 7.34 times the clipping dose.¹⁷ As a result of varying fringe contrast and average dose, we observed a varying duty cycle in the patterns of Fig. 3.

Hyperbolic phase distortion refers to the effect on pitch that is a result of the exposure beam being a spherical wave instead of an ideal plane wave. This causes the pitch to increase as features are farther from the mirror/substrate axis.^{8,18} Ferrera *et al.* showed that one can calculate the pitch as a function of position.¹⁸ We calculated that our Lloyd's mirror setup causes the pitch to vary by only $\sim 0.05\%$ over a 1 cm^2 area.

The pattern uniformity into the resist is affected by standing waves. Standing waves are an intensity modulation traveling into the photoresist. They are caused by interference between the incident beam and reflections from the bottom surface of the photoresist. It has been shown that a proper choice of an antireflection coating can minimize the effects of standing waves.¹² Using a software simulation developed by Walsh,¹⁹ we calculate the reflection from the bottom of our photoresist to be 0.69% for 200 nm of ARC and 2.82% for 303.1 nm of ARC.

Future work should focus on tool stability and reliability. Currently, the drive current of the laser is constant, but there has been no effort to stabilize the power of the laser, which has been observed to drift over the exposure time (at 42.5 mA drive current, starting intensity at the center of the v-block was $136.9 \text{ }\mu\text{W}/\text{cm}^2$ and drifted to $142.0 \text{ }\mu\text{W}/\text{cm}^2$ over 8 min). The lack of constant power limits the estimation of the exposure time and leads to different outcomes for exposures of the same duration.

The critical result of this article is the ability to fabricate large-area ($\sim \text{cm}^2$) periodic nanostructures with a simple, compact, low-cost tool. We have demonstrated that wavelength-stabilized blue laser diodes have sufficient temporal coherence to pattern greater than 1 cm^2 continuous areas. Also, we have shown that spatially coherent beams can be formed in a simple and compact way using a lens-tube-integrated spatial filter. Notably, we have been able to keep the cost of the tool below 6000 USD.

ACKNOWLEDGMENTS

The authors would like to acknowledge the contributions of Tim Savas for discussions of laser diodes, Jim Daley for clean room and SEM assistance, and Tom O'Reilly for discussions of spatial filtering. Funding for this project was provided by the Singapore-MIT Alliance and the Air Force Office of Scientific Research under Grant No. FA9550-08-1-0379.

¹S. R. J. Brueck, Proc. IEEE **93**, 1704 (2005).

²Y. S. Jung and C. A. Ross, Nano Lett. **7**, 2046 (2007).

³X.-Z. Chen and H.-Y. Li, Chin. Phys. Lett. **24**, 2830 (2007).

⁴R. Menon, H. Y. Tsai, and S. W. Thomas III, Phys. Rev. Lett. **98**, 043905 (2007).

⁵T. L. Andrew, H. Y. Tsai, and R. Menon, Science **324**, 917 (2009).

- ⁶E. Lamers, X. F. Walboomers, M. Domanski, J. te Riet, F. C. M. J. M. van Delft, R. Luttge, L. A. J. A. Winnubst, H. J. G. E. Gardeniers, and J. A. Jansen, *Biomaterials* **31**, 3307 (2010).
- ⁷I. Byun and J. Kim, *J. Micromech. Microeng.* **20**, 055024 (2010).
- ⁸M. Walsh, Ph.D. thesis, MIT, 2004.
- ⁹C. P. Fucetola, H. Korre, and K. K. Berggren, *J. Vac. Sci. Technol. B* **27**, 2958 (2009).
- ¹⁰C. E. Wieman and L. Hollberg, *Rev. Sci. Instrum.* **62**, 1 (1991).
- ¹¹G. J. Steckman, W. Liu, R. Platz, D. Schroeder, C. Moser, and F. Haver-mayer, *IEEE J. Sel. Top. Quantum Electron.* **13**, 672 (2007).
- ¹²M. L. Schattenburg, R. J. Aucoin, and R. C. Flemming, *J. Vac. Sci. Technol. B* **13**, 3007 (1995).
- ¹³T. B. O'Reilly and H. I. Smith, *J. Vac. Sci. Technol. B* **26**, 128 (2008).
- ¹⁴Warning: Use of TMAH poses a serious chemical hazard and should only be used with appropriate protective measures.
- ¹⁵C. Lin, C. Yang, J. Ger, J. Deng, and D. Hung, *Clin. Toxicol.* **48**, 213 (2010).
- ¹⁶Ondax, Inc., www.ondaxinc.com
- ¹⁷T. B. O'Reilly and H. I. Smith, *J. Vac. Sci. Technol. B* **26**, 2131 (2008).
- ¹⁸J. Ferrera, M. L. Schattenburg, and H. I. Smith, *J. Vac. Sci. Technol. B* **14**, 4009 (1996).
- ¹⁹M. Walsh, MS thesis, MIT, 2000.